An MCP based detector array with integrated electronics

Langstaff, David

Published in:
International Journal of Mass Spectrometry

DOI:
10.1016/S1387-3806(01)00578-4

Publication date:
2002

Citation for published version (APA):
Langstaff, D. (2002). An MCP based detector array with integrated electronics. *International Journal of Mass Spectrometry*, *215*(1-3), 1-12. https://doi.org/10.1016/S1387-3806(01)00578-4

An MCP based detector array with integrated electronics

DR. D.P.Langstaff
University of Wales, Aberystwyth, UK

Abstract

Various position sensitive readout systems for microchannel plates are considered. A discrete anode detector with 192 channels and integrated data acquisition electronics developed at the University of Wales, Aberystwyth is presented. Details of the custom silicon circuit which performs data acquisition in the device are given, together with key performance indicators. An example application of the detector enhancing the performance of a GCMS measurement is given. The next generation of detector currently under development is briefly introduced.

Keywords

Microchannel plate, multi-anode, array detector.

1. Introduction

The microchannel plate (MCP) is a versatile and powerful detector for ions, electrons, and photons with energies ranging from UV to X-Ray [1]. The impact of an ion, electron or photon on the front face of the MCP gives rise to secondary electrons inside the body of the MCP which results in an avalanche multiplication process leading to a pulse of up to 10^7 electrons emerging from the rear face of the MCP. By the use of a suitable collection system for these electrons, the position of the original impact on the front surface of the MCP may be determined to within a few microns.

The methods of determining the position of ion impact fall into three basic categories: Discrete anode and coincidence arrays [2-11]; Charge division [12-25]; and Optical imaging detectors [26-34]. As will be seen, each of these detection techniques makes a different trade-off in terms of performance, component count and complexity.

1.1. Charge Division Detectors

Position Sensitive Detectors based on charge division techniques give a continuous variation in output depending on the position of the event. Charge division detectors fall into three categories: Resistive anode and capacitive charge division, [13, 14, 19, 20, 23, 25, 35]; Delay line techniques [22, 26, 36-40]; and Shaped anodes [21, 41-44].

They have the advantage of low component count, requiring only 2 sets of electronics for a 1-dimensional detector and 4 sets for a 2-dimensional detector. Against this, they suffer from the limitation in maximum count rate that they can only cope with single events occurring within the time frame of the detector electronics.

1.2. Discrete multi-anode detectors

Multi-anode detectors are conceptually the simplest imaging devices employed with MCPs. An array of anodes is placed within proximity focus of the rear face of the MCP stack in vacuum or is deposited directly on the rear face of the MCP [3-5, 7, 8, 45-48]. Each anode is connected to an electronics channel comprising a charge sensitive amplifier, discriminator and counter.

The spatial resolution of the detector is limited only by the size of the spacing of the anodes (assuming this is greater than the pore spacing of the MCP). High count rates are achievable, limited only by the performance of the MCP.

Conventional multi-anode arrays suffer from the disadvantage of requiring a large number of electronic components due to the discrete electronics required for each anode and also from cross talk between the anodes [49]. Stray capacitances on each channel are of the order of 10pF with a cross coupling capacitance of 0.5pF between adjacent channels, resulting in peak signals of the order of 20mV with 1mV of cross coupled signal appearing on adjacent electrodes. In conventional multi-anode arrays the channel to channel crosstalk is the limiting factor in the performance of the detector. In addition to the performance limits imposed by stray capacitance, the multi-way feedthrough needed to connect the detector in the vacuum system to the external electronics system is a problematic and expensive component.

1.3. Coincidence arrays

Coincidence arrays are an attempt to reduce the component count inherent in multi-anode detectors by connecting the anodes to the amplifiers in such a way as the position of the event is encoded by simultaneous pulses from two amplifiers.

The performance cost of this reduction in component count is manifested in a reduction in the maximum count rate that the detector can cope with. The detector responds badly to the case of two events occurring within the time resolution of the amplifiers and coincidence detector, effectively giving a random position for one event occurring. Thus the maximum count rate for the coincidence detector will be determined by the time required for the electronics to decode and output the position of the event and reset itself ready for the next event.

At high count rates the random events caused by pulse 'pile-up' will manifest themselves as noise spread across the array, thus a coincidence detector has a low 'intra-specular' dynamic range, despite achieving a respectable dynamic range for single peaks.

1.4. Integrated multi-anode devices

By integrating the charge amplifier and discriminator circuits onto a piece of silicon together with the collection anodes, the problems associated with crosstalk can be greatly reduced in a multi-anode detector. By putting some of the data acquisition electronics in the vacuum system, right alongside the MCP, it is possible to arrange that only low impedance logic level signals have to pass through the vacuum envelope; additionally, by accumulating counts in the data acquisition device, the feedthrough requirements may be greatly reduced. The other advantage of an integrated device is that the high component count traditionally associated with multi-anode devices is greatly reduced, the Aberystwyth detector contains approximately 64,000 devices on a single piece of silicon measuring approximately 5mm × 15mm.

One such device is due to Hatfield & Hicks (UMIST, UK) [50, 51]. This has up to 29 channels on a pitch of 160μm and has been fabricated and tested in a number of applications.

The detector presented here is an integrated multi-anode device and differs from the Hatfield & Hicks detector in several important respects, notably in that this detector has 192 channels on a pitch of 25µm. In addition, the sensor circuits used on this device are self resetting [52], requiring no global clocks, which simplifies control of the array.

2. The Aberystwyth Detector

The Aberystwyth Charge Sensitive Detector array comprises a number of custom silicon integrated circuits mounted on a ceramic substrate in proximity to the rear face of an MCP. Each detector chip contains 192 channels, or pixels, on a pitch of 25µm. Each channel has a metal anode to collect the electrons as they emerge from the MCP; a charge sensitive amplifier to produce a digital signal in response to the electron pulse and an 8-bit counter associated with it to accumulate the counts as they arrive and circuitry to read out the data sequentially from all channels in the array. The spacing of the anodes was chosen to fit in with the geometry of a typical mass spectrometer having a minimum source slit width of 25µm and a magnification close to unity. The collection anodes are furnished with a secondary electrode allowing charge to be injected from an external source, this is invaluable in allowing the circuit to be tested once silicon fabrication is complete so that good devices may be selected for assembly into the detector modules. A floorplan of the device is shown in Figure 1, showing the layout of the principal components and their relative sizes.

The silicon detector chip was fabricated on a 3µm CMOS process by Hughes Microelectronics Europa Ltd. In order to reduce the stray capacitance associated with the collection anodes a special processing step was specified in the CMOS process where the normal dielectric layer underneath the uppermost metal layer in the circuit was replaced with a thick layer of polyimide material, this reduced the capacitance of each anode to approximately 0.2pF, with a cross coupling capacitance of 0.003pF. The low value of anode capacitance and even lower cross coupling capacitance results in a large signal presenting itself at the input to the on-chip charge sensitive amplifier. Simulations predict that a voltage

pulse of about 0.1V will result from 10^5 electrons emerging from the MCP and landing on the collection anode.

An important feature of any MCP readout device is its ability to withstand transients appearing on the input. The MCP is an avalanche device and it is possible for output pulses much larger than normal to be produced, particularly during initial run-up of the MCP. The input circuits on the Aberystwyth detector have been designed with protection devices such that excess charge on the collection anode is conducted away to ground before it can damage the sensitive circuitry of the charge sensitive amplifier.

The circuit has been designed such that an arbitrary number of detector chips may be abutted together on a substrate behind the MCP, allowing for long focal plane detectors to be built, limited only by the size of MCPs available (currently approximately 100mm). The output from the counters on the detectors is presented via an 8-bit port and is read into a PC by means of a simple interface based around the 8255 Peripheral Interface Adapter circuit. A number of detectors have been built and tested in a number of different instruments. A summary of results obtained is presented here.

2.1. Peak shape & Spatial resolution

Initial *in vacuuo* testing of the device was done in a VG/Micromass Autospec mass spectrometer, using the background residual gas in the machine. The detector was positioned at approximate location of the focal plane of the instrument, behind the conversion dynode of the existing photomultiplier detector in the machine as shown in Figure 2. When the machine is used with the conventional photomultiplier detector, the conversion dynode is at a potential of –40kV, ions passing through the collector slit are accelerated onto the aluminium surface of the dynode and cause secondary electrons to be liberated. These secondary electrons impinge upon the scintillator where photons are created which travel down the light guide to be converted back to an electrical signal and amplified by an avalanche photomultiplier. When the conversion dynode potential is removed, the incoming ions impinge upon the front face of the MCP and are detected by the array detector. Positioning the detector in such a way

enabled the beam to be switched between the two detectors simply by switching the supply to the conversion dynode. A deflection lens assembly (not shown in diagram) is positioned in front of the MCP allowed the incoming beam of ions to be steered across the array independently of the ion optics of the rest of the instrument. The machine was aligned and optimised using the photomultiplier before switching the beam onto the array detector, when the peak in Figure 3 was obtained. The peak shown is at mass 32 and corresponds to $^{16}O_2^+$. The Full Width Half Maxima (FWHM) of a number of peaks were measured and the average found to be 82μm or just over 3 detector channels.

2.2. Noise Floor and Maximum Count Rate

By turning off the ion source in the instrument it is possible to determine the dark count rate, or noise floor, of the detector. This was measured and found to be approximately 3×10^{-4} counts per second per channel, by turning off the MCP supply potential it was confirmed that all of this noise was arising in the MCP.

By using the array detector in the configuration with the existing photomultiplier based detector it is possible to determine the linearity of the array detector and in particular the maximum count rate that maybe obtained from it. Three peaks of widely differing amplitudes were located in the residual background atmosphere of the instrument. These peaks arise from the oil used in the diffusion pumps of the instrument and can be expected to remain constant over a long period of time. The amplitudes of these peaks were recorded on both the photomultiplier and the array detector as their amplitudes were varied over a wide range by adjusting the ion source of the instrument. The result is shown in Figure 4, where the measurement points are plotted alongside a curve giving the theoretical response of a paralyzable counter[53]. In this case the modified count rate of the counter is given by the equation:

$$\lambda' = \lambda \cdot e^{-\lambda \cdot \tau}$$

where λ' is the modified count rate, λ the original count rate and τ the dead time of the detector. By fitting this theoretical curve to the observed data, it was found that the value of τ and hence the dead time of each channel is approximately 16 μs. It should be noted that this dead-time is due to the MCP and agrees closely with the quoted maximum count rate for the MCP adjusted for the area of one of the collection anodes. Combining this result with the dark noise result gives an ion counting detector which is linear over approximately 7 orders of magnitude, limited at each end of its performance scale by current MCP technology.

2.3. Comparison with other detectors

The performance of the Aberystwyth Integrated Multianode detector is compared with examples of MCP readout systems in Table 1. It can be seen that the performance attained by the Aberystwyth detector equals or surpasses that of other readout systems, particularly as regards to the dynamic range of the system, where the MCP becomes the limiting factor in performance.

3. Applications

The versatility and range of uses of this detector are very broad indeed. As was seen above, the dynamic range of the device is limited only by the current state of microchannel plate performance and other features of the detector give it unique benefits when used in several application areas. This section illustrates the benefits offered by the detector by showing how the imaging ability of the detector enables differentiation between different elutants from a Gas Chromatography Mass Spectrometry (GCMS) analysis [56].

In applications where Gas Chromatography is combined with Mass Spectrometry (GCMS) there is a requirement for high sensitivity detection combined with high resolution. This is particularly true in the case of trace analysis of environmental contaminants, such as polychlorinated dioxins, furans and biphenyls, and also in the detection of drugs of abuse and performance enhancing substances in sport. In these applications the only available technique

for analysis is a mode of operation known as Selective Ion Recording (SIR). In the SIR technique, the mass spectrometer is set to record ions from one mass at a time, rather than scanning a spectrum from a range of masses across a single point detector. In this way, the detector may operate at maximum sensitivity, however, the technique is susceptible to interferences caused by contributions from peaks of similar mass to the measured peak entering the detector.

In order to confirm the presence of these interferences, it is possible, in some cases, to switch between two or more ions and perform isotope ratio measurements on these. However, in cases where interference is suspected, there is often no information in the SIR data to determine the extent or cause of the interference. Mass profile scanning [57], which employs a series of short scans across the width of the peak, can provide more information about possible interferences, but at a loss of sensitivity.

A typical SIR chromatogram obtained from a sample of a doping control standard at mass 448.3192 Da is shown in Figure 5. This chromatogram was obtained using the existing photomultiplier fitted to the machine and the mass determined by using the standard machine calibrations and operating conditions. Of particular interest were the peaks in the magnified area (4 & 6), which were thought to be due to interference arising from side lobes of peaks of ions near to the target mass.

A routine was written for the detector array control program which would repeatedly take samples from the array, storing each sample onto disk together with the value of the PCs real time clock at the time of the sample, allowing a sequence of spectra taken over time to be accumulated.

The experiment was repeated using the detector array with the control program set to take a series of readings over a period of several minutes. Once the readings had been taken, the results were plotted as a 3D plot as shown in Figure 6. In this plot, time is plotted along the x-axis, the mass of the ion is plotted along the y-axis into the page and the number of counts

plotted on the z-axis. Although the array detector has not been accurately calibrated to allow conversion from channel number to mass, rough calculations show that under these conditions, the mass calibration is approximately 0.001Da/channel.

By viewing the 3D plot from above, a contour plot is formed as shown in Figure 7, the presence of the interference peaks (4, 5 & 6) may be readily confirmed. By observing the peaks (not shown on plots) due to the carrier gas in the GC column, which remain constant over time, it was possible to confirm that the shift in centre of mass of peaks 4,5&6 was indeed due to interference from unwanted species rather than machine drift.

4. Conclusions & Further Directions

The detector presented here represents a major advance on the performance attainable from other MCP readout techniques. The integration of the first stage of data acquisition circuitry alongside the collection anodes, inside the vacuum system, offers many advantages in terms of both detector performance and also system integration. The silicon integrated circuits containing the data acquisition circuitry have proved to be vacuum compatible, work is currently being carried out on an electron spectrometry application where a detector module has been pumped to 10^{-9} Torr and 'sniffed' with a mass spectrometer head which revealed no serious outgassing. The circuit has also proved electrically robust, withstanding both normal operation and a number of flashover type incidents within the MCP stack. Further work is planned to determine the ESD tolerance of the device.

Work is progressing on the design and construction of the next generation of detector devices at Aberystwyth. Although the project is specifically aimed at electron energy spectrometry, the detector will also find application in mass spectrometry and other fields. Advances in silicon fabrication have shrunk the feature size attainable and a process with a gate length of 0.5µm is now readily available, compared with the gate length of 3µm used in the device presented here. The smaller feature sizes attainable will result in a device with higher sensitivity to electrons, allowing the MCP to be operated at a lower potential resulting in less spreading of the peak. In addition, as the devices within the charge sensitive amplifiers are

proportionately larger compared with the minimum possible, there should be greater uniformity from channel to channel across the device. Test structures for this process are being fabricated at the time of going to press and offer the possibility of improved uniformity across the array and the fabrication of detector circuits with more pixels.

5. Bibliography and References

1. Hamamatsu Photonics K.K. 1991, Hamamatsu Photonics K.K. Electron Tube Centre: Shizuoka-ken, Japan.
2. J.G. Timothy and R.L. Bybee, Applied Optics, 1975. **14**(7): p. 1632-1644.
3. A.L. Broadfoot and B.R. Sandel, Applied Optics, 1977. **16**(6): p. 1533-8.
4. J.G. Timothy and R.L. Bybee, Proceedings of the Society of Photo-Optical Instrumentation Engineers, 1977. **116**: p. 24-32.
5. E. Kellogg, S. Murray, U. Briel, and D. Bardas, Review of Scientific Instruments, 1977. **48**(5): p. 550-3.
6. T.S. Padmore, K.M. Roberts, H.A. Padmore, and G. Thornton, Nuclear Instruments and Methods in Physics Research, 1988. **A270**: p. 582-9.
7. J. Krider, Nuclear Instruments & Methods In Physics Research Section A, 1986. **A247**(2): p. 304-308.
8. C. De Michelis, M. Mattioli, P. Monier-Garbet, J.C. Vidal, and W. Hecq, Measurement Science and Technology, 1993. **4**: p. 109-113.
9. V.P. Volkov, B.M. Glukhovskoi, N.M. Selivanchik, and I.F. Yaroshenko, Instruments And Experimental Techniques, 1991. **33**(6): p. 1372-1375.
10. J.G. Timothy, G.H. Mount, and R.L. Bybee, IEEE Transactions on Nuclear Science, 1981. **NS-28**(1): p. 689-697.
11. E. Horch, J.F. Heanue, J.S. Morgan, and J.G. Timothy, Publications Of The Astronomical Society Of The Pacific, 1994. **106**(703): p. 992-1002.
12. R. Gott, W. Parkes, and K.A. Pounds, Nuclear Instruments & Methods In Physics Research, 1970. **81**: p. 152-4.
13. M. Lampton and F. Paresce, Review of Scientific Instruments, 1974. **45**(9): p. 1098-1105.
14. W. Parkes, K.D. Evans, and E. Mathieson, Nuclear Instruments & Methods In Physics Research, 1974. **121**: p. 151-9.
15. C.D. Moak, S. Datz, F. Garcia Santibanez, and T.A. Carlson, Journal of Electron Spectroscopy and Related Phenomena, 1975. **6**: p. 151-156.
16. M. Lampton and R.F. Malina, Review of Scientific Instruments, 1976. **47**: p. 1360.
17. R.W. Wijandts van Resandt, H.C. den Harick, and J. Los, Journal of Physics, 1976. **E 9**: p. 503-9.
18. J.L. Wiza, P.R. Henkel, and R.L. Roy, Review Of Scientific Instruments, 1977. **48**(9): p. 1217-1218.
19. W. Aberth, International Journal of Mass Spectrometry and Ion Physics, 1981. **37**: p. 379-382.
20. C. Firmani, E. Ruiz, C.W. Carlson, M. Lampton, and F. Paresce, Review Of Scientific Instruments, 1982. **53**(5): p. 570-574.
21. H.E. Schwarz and J.S. Lapington, IEEE Transactions on Nuclear Science, 1985. **NS-32**(1): p. 433-7.

22. M. Lampton, O.H.W. Siegmund, and R. Raffanti, Review of Scientific Instruments, 1987. **58**: p. 2298-2305.
23. M. Clampin, J. Crocker, F. Paresce, and M. Rafal, Review of Scientific Instruments, 1988. **59**(8): p. 1269-85.
24. R.H. Brigham, R.J. Bleiler, P.J. Mcnitt, D.A. Reed, and R.H. Fleming, Review Of Scientific Instruments, 1993. **64**(2): p. 420-9.
25. P. Downie, D. Litchfield, R. Parsons, D.J. Reynolds, and I. Powis, Measurement Science & Technology, 1993. **4**(11): p. 1293-1296.
26. G.R. Riegler and K.A. More, IEEE Transactions on Nuclear Science, 1973. **NS-20**: p. 102-6.
27. B.R. Sandel and A.L. Broadfoot, Applied Optics, 1976. **15**(12): p. 3111-4.
28. B. Hedfjäll and R. Ryhage, Analytical Chemistry, 1979. **51**(11): p. 1687-90.
29. P.J. Hicks, S. Daviel, B. Wallbank, and J. Comer, Journal Of Physics E: Scientific Instruments, 1980. **13**: p. 713-715.
30. Y. Talmi and R.W. Simpson, Applied Optics, 1980. **19**(9): p. 1401-14.
31. G.J. Louter and A.N. Buijserd, International Journal Of Mass Spectrometry and Ion Physics, 1983. **50**: p. 245-57.
32. M. Parkinson, Applied Optics, 1989. **28**(11): p. 2087-96.
33. M. Raymond, G. Hall, M. Lovell, P. Sharp, C. Lewin, and P. Seller, Nuclear Instruments and Methods in Physics Research, 1994. **A348**: p. 673-677.
34. D.J. Sahnow, P.D. Feldman, S.R. Mccandliss, and E.F. Mackey, Review Of Scientific Instruments, 1994. **65**(4 Pt1): p. 813-825.
35. J. Carrico, C. Johnson, and T.A. Somer, International Journal of Mass Spectrometry and Ion Physics, 1973. **11**: p. 409-415.
36. S.E. Sobottka and M.B. Williams, IEEE Transactions on Nuclear Science, 1988. **NS-35**(1): p. 348-351.
37. J.A. Hill, J.E. Biller, S.A. Martin, K. Biemann, K. Yoshidome, and K. Sato, International Journal of Mass Spectrometry and Ion Processes, 1989. **92**: p. 211-230.
38. O.H.W. Siegmund, M. Lampton, and R. Raffanti, Proceedings of the Society of Photo-Optical Instrumentation Engineers, 1989. **1159**: p. 476-485.
39. O.H.W. Siegmund, M. Lampton, R. Raffanti, and W. Herrick, Nuclear Instruments & Methods In Physics Research, 1991. **A310**: p. 311-6.
40. O.H.W. Siegmund, R. Raffanti, J. Stock, W. Herrick, and M. Lampton. *Conference on Photoelectronic Image Devices*. 1991. London.
41. H.O. Anger: U.S. Patent 3,209,201.
42. C. Martin, P. Jelinsky, M. Lampton, R.F. Malina, and H.O. Anger, Review Of Scientific Instruments, 1981. **52**(7): p. 1067-1074.
43. O.H.W. Siegmund, S. Clothier, J. Thornton, J. Lemen, R. Harper, I.M. Mason, and J.L. Culhane, IEEE Transactions on Nuclear Science, 1983. **NS-30**(1): p. 503-7.
44. J.S. Lapington and H.E. Schwarz, IEEE Transactions on Nuclear Science, 1986. **33**(1): p. 288-92.
45. K. Oba, M. Sugiyama, Y. Suzuki, and Y. Yoshimura, IEEE Transactions on Nuclear Science, 1979. **NS-26**: p. 346.
46. H. Brockhaus and A. Glasmachers, Ieee Transactions On Nuclear Science, 1992. **39**(4): p. 707-711.
47. J.O. McGarity, A. Huber, J. Pantazis, M.R. Oberherhardt, D.A. Hardy, and W.E. Slutter, Review of Scientific Instruments, 1992. **63**(3): p. 1973-7.

48. A.J. Bird, Z. He, and D. Ramsden, Nuclear Instruments & Methods In Physics Research Section a- Accelerators Spectrometers Detectors and Associated Equipment, 1994. **348**(2-3): p. 668-672.
49. M. Liptak, IEEE Transactions on Nuclear Science, 1984. **NS-31**(1): p. 780-785.
50. P.J. Hicks and J.V. Hatfield, *Charged Particle Multidetector*. 1989, UNIV MANCHESTER (GB): U.K. Patent WO9003043 GB89 01067.
51. J.V. Hatfield, J. Comer, T.A. York, and P.J. Hicks, Review Of Scientific Instruments, 1992. **63**(1 Pt2A): p. 792-796.
52. K. Birkinshaw, *Charge Sensor and Spectrometers Incorporating it*. 1991, VG INSTR GROUP (GB): U.K. Patent WO9100612.
53. A. Sharma and J.G. Walker, Review Of Scientific Instruments, 1992. **63**(12): p. 5784-5793.
54. J.V. Hatfield, S.A. Burke, J. Comer, F. Currell, J. Goldfinch, T.A. York, and P.J. Hicks, Review Of Scientific Instruments, 1992. **63**(1): p. 235-240.
55. J.G. Timothy and R.L. Bybee, S.P.I.E., 1981. **265**: p. 93-105.
56. J. Hart, R. Bordoli, R. Bateman, K. Birkinshaw, and D. Langstaff. *The 45th ASMS Conference on Mass Spectrometry and Allied Topics*. 1997. Palm Springs, California, USA.
57. H. Tong, M. Gross, D. Giblin, S. Monson, L. Huang, C. Moore, J. Moncur, and P. Ryan, Chemosphere, 1992. **25**(1-2): p. 21-24.

List of figures

Detector Type	Reference	Spatial resolution	Number of channels	Maximum count rate (channel)	Maximum count rate (array)	Dynamic range	Notes
		μm		counts second^{1}	counts second^{1}		
Aberystwyth (Integrated Multianode)		**25**	**192/chip**	**10^4 †**	**4×10^6**	**$>10^5$**	**2 chip module demonstrated (384 channels)**
Other Integrated multianode	[54]	160	32/chip				4 chip module demonstrated (128 channels)
Discrete multianode	[2]	50	96	10^4 †	10^6		High component count for readout Performance limited by cross coupling
Coincidence array (MAMA)	[55]	25	1024	2×10^3	2×10^6	100	Pulse pile-up at high count rates limits dynamic range
Charge division (Resitive Anode / Capacitive division / Coded Anode)	[13] [12]	400	64	10^4	7×10^5	10^4	Resolution limited by noise Pulse pile-up at high count rates causes ghosting
Optical Imaging (photodiode)	[30]	25	1024	5×10^5	1×10^7	500	Not pulse counting at high rates

† Count rate limited by MCP

Table 1 Comparison of different MCP based detectors

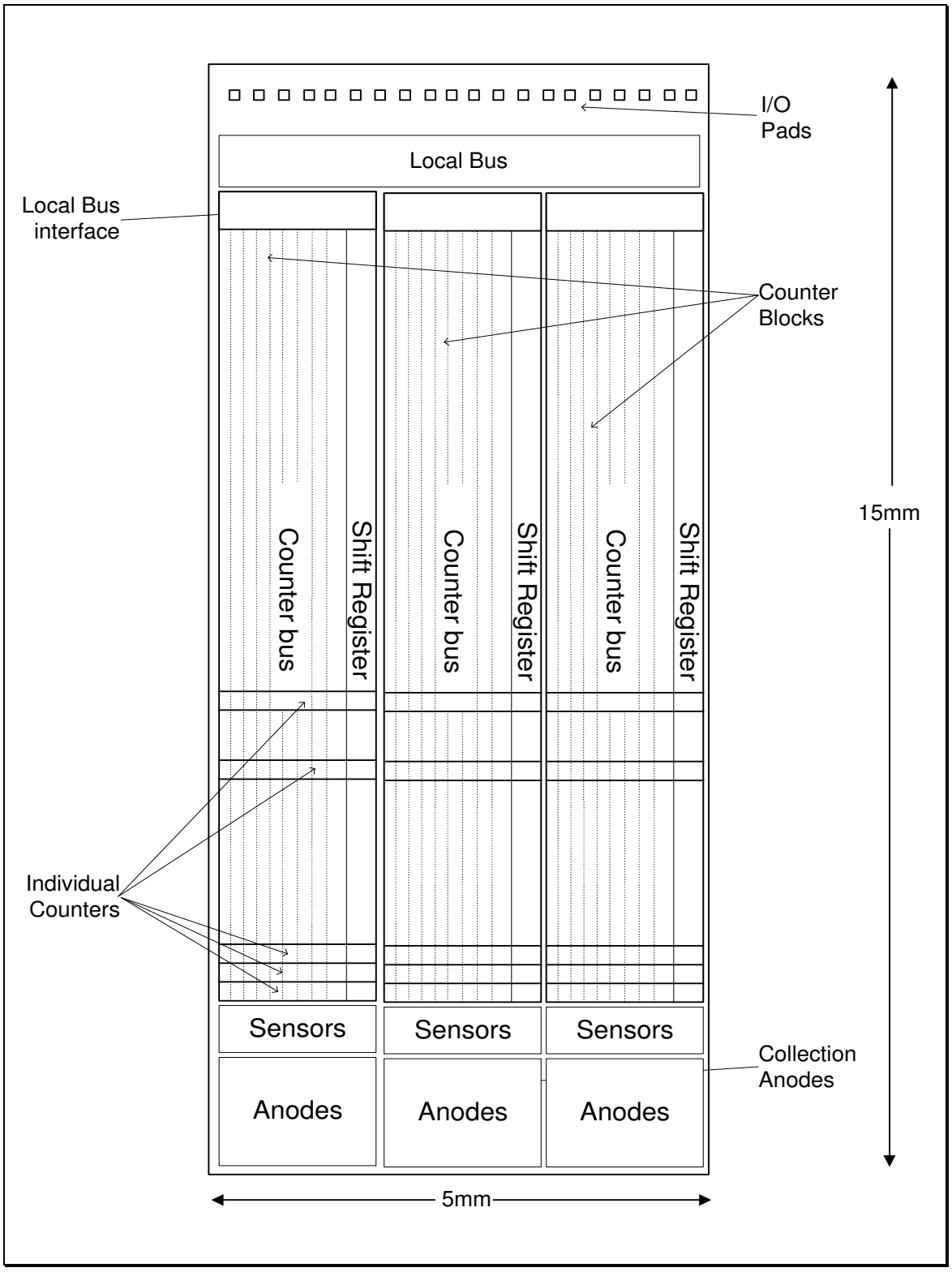

Figure 1 Floorplan of array detector circuit

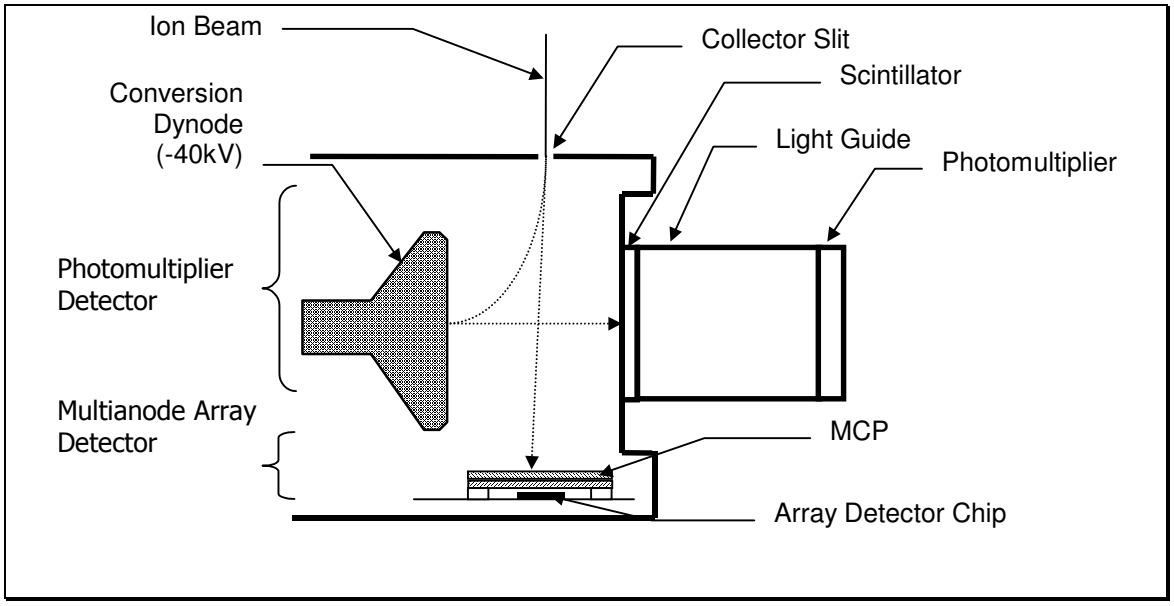

Figure 2 Mounting the array detector with the existing photomultiplier

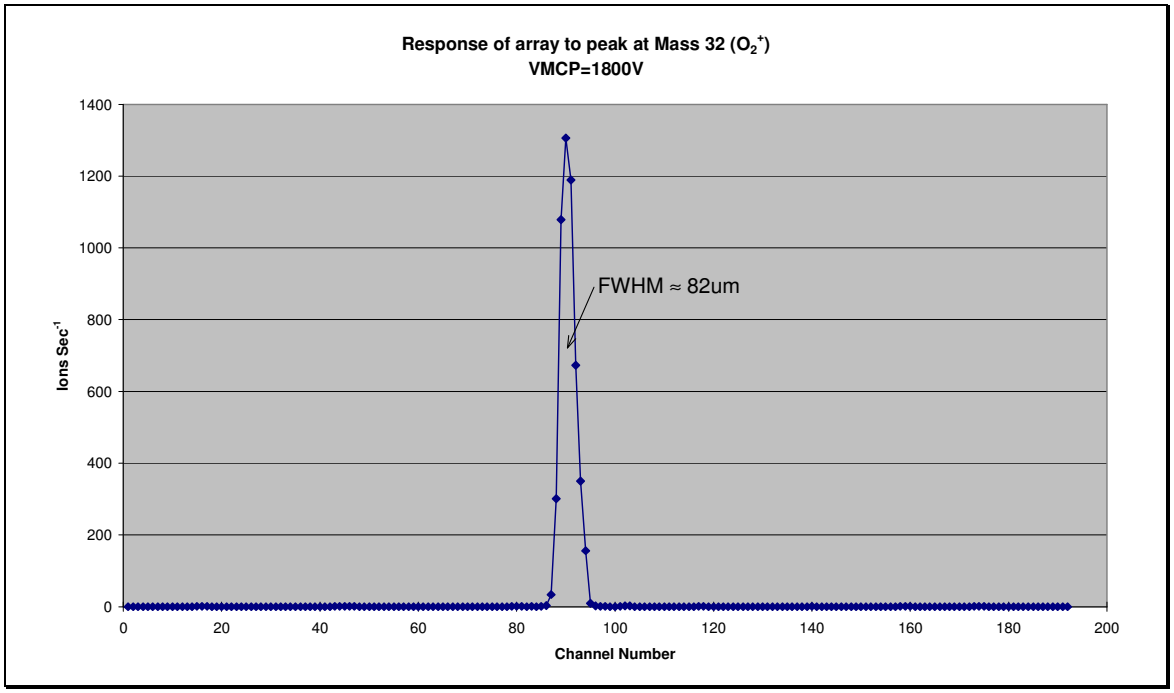

Figure 3 Image of peak at mass 32

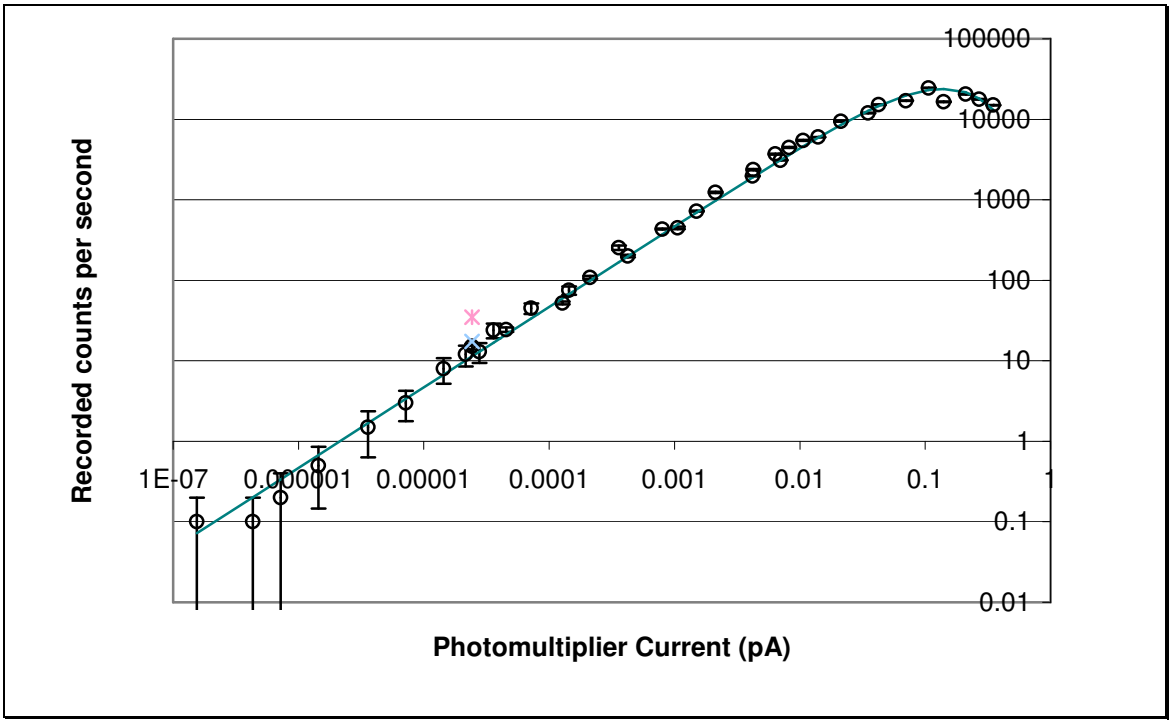

Figure 4 Comparison of Array detector with Photomultiplier

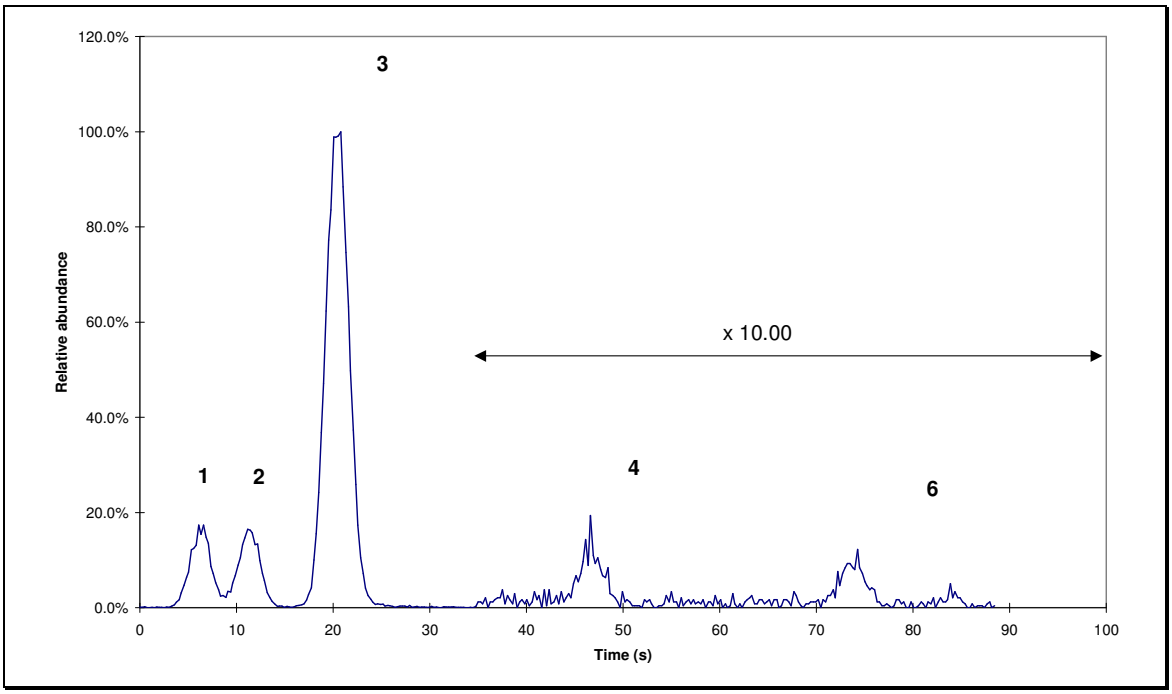

Figure 5 Chromatogram of 448.3192 acquired using conventional detector

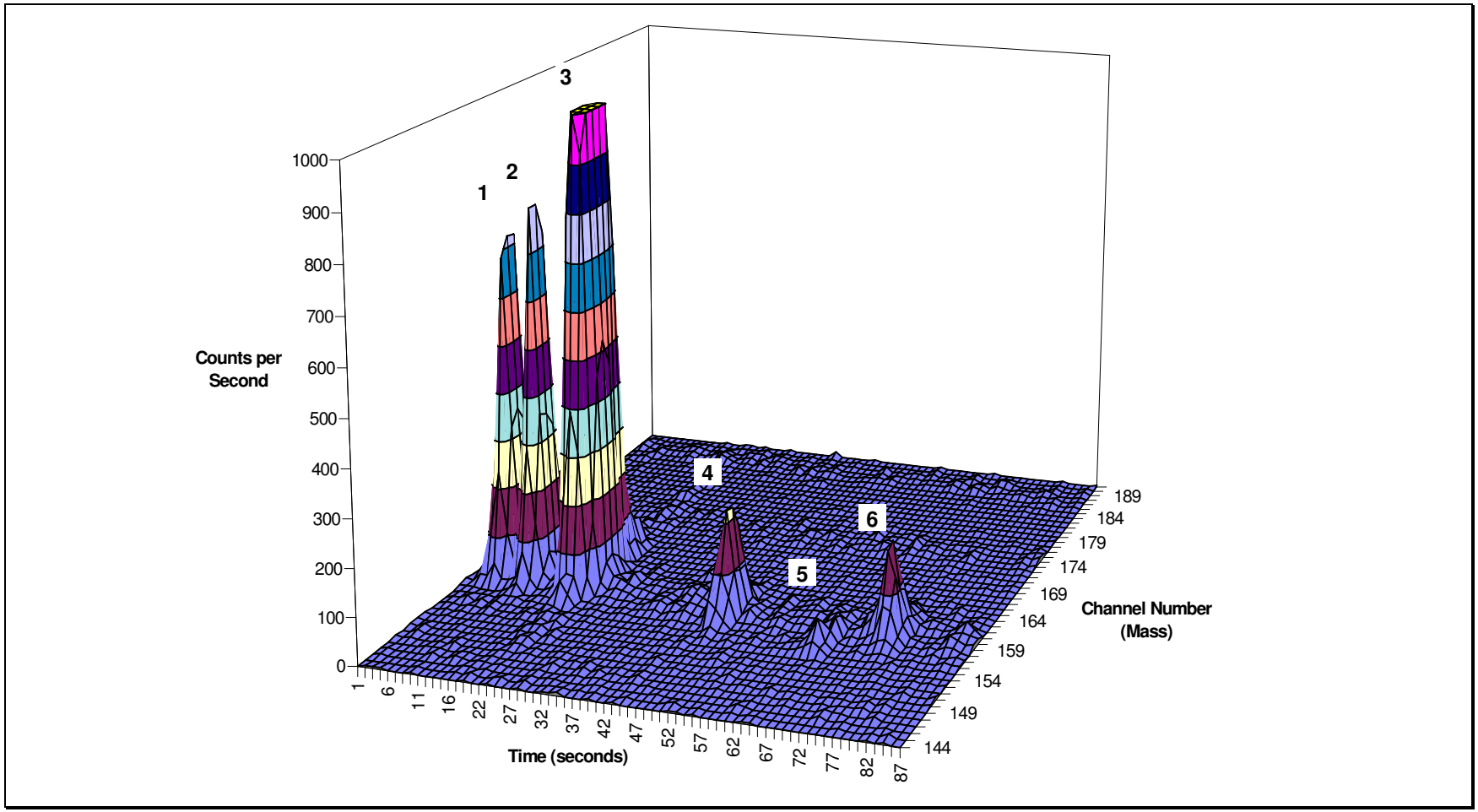

Figure 6 Chromatogram of 448.3192 acquired using array detector

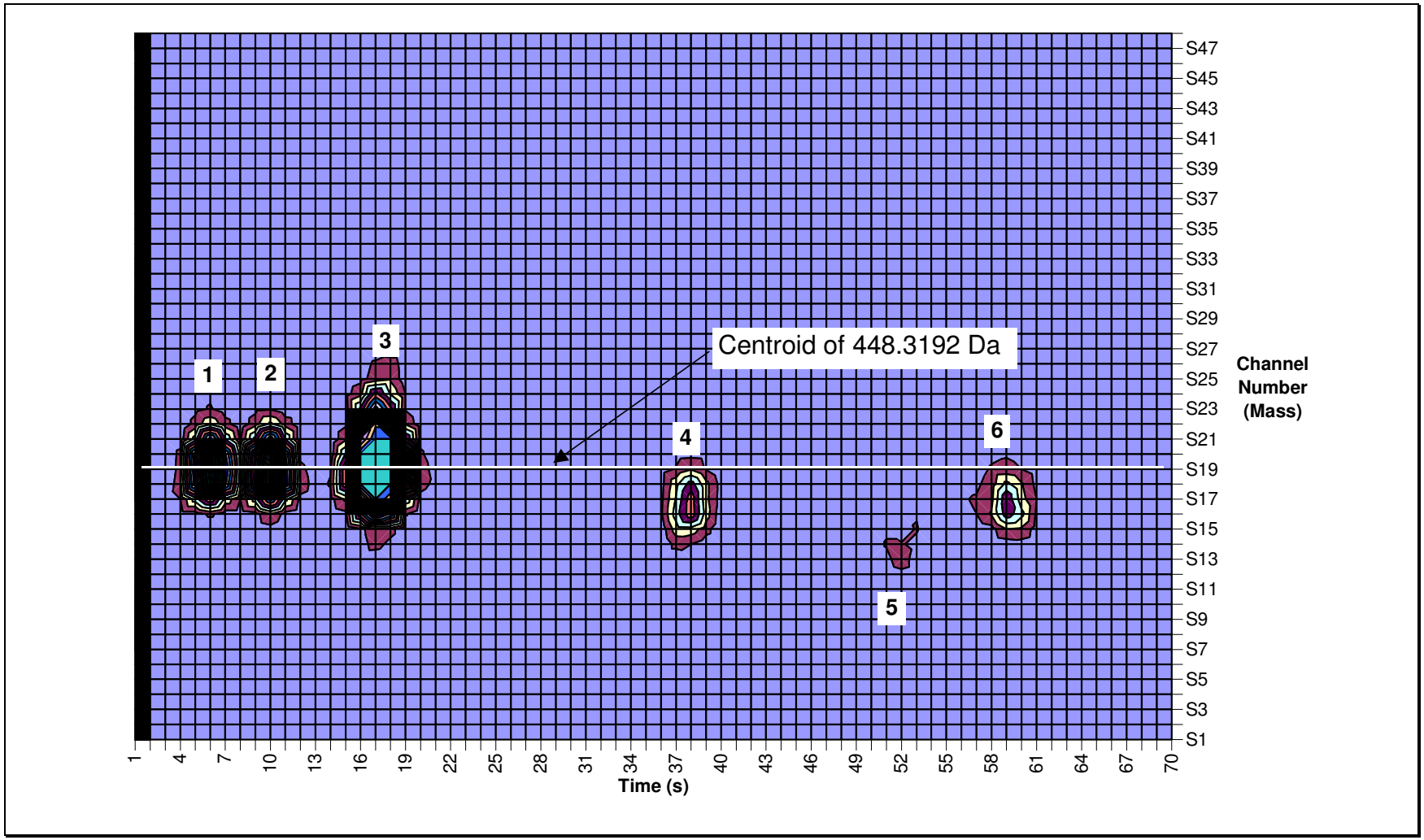

Figure 7 Contour plot of chromatogram at 448.3192 Da